Growth of Polycrystalline Tubular Silicon Carbide Yajima-Type Reaction at the Vapor−Solid Interface

Chia-Hsin Wang,[†] Huang-Kai Lin,[†] Tsung-Ying Ke,[‡] Thomas-Joseph Palathinkal,[‡] Nyan-Hwa Tai,[‡] I-Nan Lin,[§] Chi-Young Lee,[‡] and Hsin-Tien Chiu*[,†]

Department of Applied Chemistry, National Chiao Tung University, Hsinchu, Taiwan 30050, ROC, Department of Materials Science and Engineering and Center for Nanotechnology, Materials Science and Microsystems, National Tsing Hua University, Hsinchu, Taiwan 30043, ROC, and Department of Physics, Tamkang University, Taipei, Taiwan 25137, ROC

Received April 3, 2007. Revised Manuscript Received May 26, 2007

Polycrystalline tubular SiC on Si is prepared by reacting $MeSiHCl_2$ vapor and Ca thin film on Si at 773−923 K followed by heat treatment at 1273 K. The reaction is a solvent-free Yajima-type process taking place at the vapor−solid interface. The products phase-segregate into a cable-like radial heterostructure composed of a core of $CaCl_2$ and a shell of SiC_xH_y. After removal of the $CaCl_2$ core, the layer of polycrystalline SiC tubes on Si can emit electrons at a low applied field of 2.5 V/μm with a current of 10 μA/cm^2.

Introduction

Silicon carbide is an important semiconductor material for high temperature, high power, and high frequency applications in demanding environments.[1] Therefore, fabrication of silicon carbide into nanometer scale devices has received considerable attention. To date, many kinds of silicon carbide nanostructures have been successfully fabricated, including nanoboxes, hollow nanospheres, nanorods, nanowires, and nanocables.[2−5] But, there were only limited reports on the synthesis of tubular silicon carbide nanostructure.[6−8] Drawbacks of these approaches include low yields, low crystallinity, and difficulty to remove templates. Here, we demonstrate that by using simple vapor−solid reaction growth (VSRG) methodology,[9−11] high yield synthesis of large area polycrystalline tubular SiC on Si substrates can be achieved by employing methyldichlorosilane, $MeSiHCl_2$, to react with Ca thin films on Si(100) wafers at relatively low temperatures. The reaction is an improved Yajima-type reaction carried out in a solvent-free condition.[12] One-dimensional β-SiC fibers prepared from the Yajima process can be used for many advanced structural applications.[13] In this study, potential application of the tubular SiC as an efficient field emitting material will be explored.[14−15]

Experimental Section

A hot-wall reactor composed of a Lindberg HTF55122A tube furnace and a 27 mm diameter quartz tube was used. In a typical reaction, Ca powders (Alfa Aesar 99.5%, 0.30 g, 7.5 mmol) in a 10 cm quartz boat were placed at a distance 5 cm upstream away from the center of the reactor. Another quartz boat loaded with Si(100) substrates was placed at 25 cm away from the center, which was located just outside the furnace and at 430 K. Evaporation of Ca was performed at 973 K under vacuum for 1 h so that Ca thin films deposited on the Si substrates. Then, under 1 atm of Ar, the Ca coated Si substrates were pushed into the reactor center. Under the assistance of a constant flow of Ar (10 sccm), $MeSiHCl_2$ at 255 K was evaporated into the reactor. The reaction was carried out at 773−923 K for 12 h to generate a precursor coating. Finally, the precursor coating was heated at 1273 K for 1 h under vacuum to offer samples of a layer of yellow thin film on Si.

Scanning electron microscopy (SEM) and energy dispersive X-ray (EDX) spectroscopic data were collected using a JEOL JSM-

* Corresponding author. Fax: 886-3-5723764. Tel: 886-3-5712121, ext. 56504. E-mail: htchiu@faculty.nctu.edu.tw.
[†] National Chiao Tung University.
[‡] National Tsing Hua University.
[§] Tamkang University.

(1) Fissel, A.; Schroter, B.; Richter, W. *Appl. Phys. Lett.* **1995**, *66*, 3182.
(2) Wang, C.-H.; Chang, Y.-H.; Yen, M.-Y.; Peng, C.-W.; Lee, C.-Y.; Chiu, H.-T. *Adv. Mater.* **2005**, *17*, 419.
(3) Dai, H. J.; Wong, E.; Lu, Y. Z.; Fan, S. S.; Lieber, C. M. *Nature* **1995**, *375*, 769.
(4) (a) Pan, Z. W.; Lai, H. L.; Au, F. C. K.; Duan, X. F.; Zhou, W. Y.; Shi, W. S.; Wang, N.; Lee, C. S.; Wong, N. B.; Lee, S. T.; Xie, S. S. *Adv. Mater.* **2000**, *12*, 1186. (b) Ye, H.; Titchenal, N.; Gogotsi, Y.; Ko, F. *Adv. Mater.* **2005**, *17*, 1531.
(5) Li, Y.; Bando, Y.; Golberg, D. *Adv. Mater.* **2004**, *16*, 93.
(6) Sun, X. H.; Li, C. P.; Wong, W. K.; Wong, N. B.; Lee, C. S.; Lee, S. T.; Teo, B. K. *J. Am. Chem. Soc.* **2002**, *124*, 14464.
(7) Hu, J. Q.; Bando, Y.; Zhan, J. H.; Golberg, D. *Appl. Phys. Lett.* **2004**, *85*, 2932.
(8) Wang, H.; Li, X.-D.; Kim, T.-S.; Kim, D.-P. *Appl. Phys. Lett.* **2005**, *86*, 173104.
(9) Huang, C.-H.; Chang, Y.-H.; Lee, C.-Y.; Chiu, H.-T. *Langmuir* **2006**, *22*, 10.
(10) Yen, M.-Y.; Chiu, C.-W.; Shia, C.-H.; Chen, F.-R.; Kai, J.-J.; Lee, C.-Y.; Chiu, H.-T. *Adv. Mater.* **2003**, *15*, 235.
(11) Hsia, C.-H.; Yen, M.-Y.; Lin, C.-C.; Chiu, H.-T.; Lee, C.-Y. *J. Am. Chem. Soc.* **2003**, *125*, 9940.
(12) (a) Yajima, S.; Hayasht, J.; Hasegawa, Y.; Iimura, M. *J. Mater. Sci.* **1978**, *13*, 2569. (b) Hasegawa, Y.; Iimura, M.; Yajima, S. *J. Mater. Sci.* **1980**, *15*, 720. (c) Hasegawa, Y.; Okamura, K. *J. Mater. Sci.* **1983**, *18*, 3633.
(13) (a) Miller, J. H.; Liaw, P. K.; Landes, J. D. *Mater. Sci. Eng. A* **2001**, *317*, 49. (b) Miriyala, N.; Liaw, P. K.; Mchargue, C. J.; Snead, L. L. *J. Nucl. Mater.* **1998**, *253*, 1. (c) Liaw, P. K.; Hsu, D. K.; Yu, N.; Miriyala, N.; Saini, V.; Jeong, H. *Acta Mater.* **1996**, *44*, 2101.
(14) Yoshimoto, T.; Yokogawa, N.; Iwata, T. *Jpn. J. Appl. Phys.* **2006**, *45*, L482.
(15) Evtukh, A. A.; Klyui, N. I.; Litovchenko, V. G.; Litvin, Y. M.; Kprneta, O. B.; Puzikov, V. M.; Semenov, A. V. *Appl. Surf. Sci.* **2003**, *215*, 237.

10.1021/cm070925e CCC: $37.00
Published on Web 07/04/2007

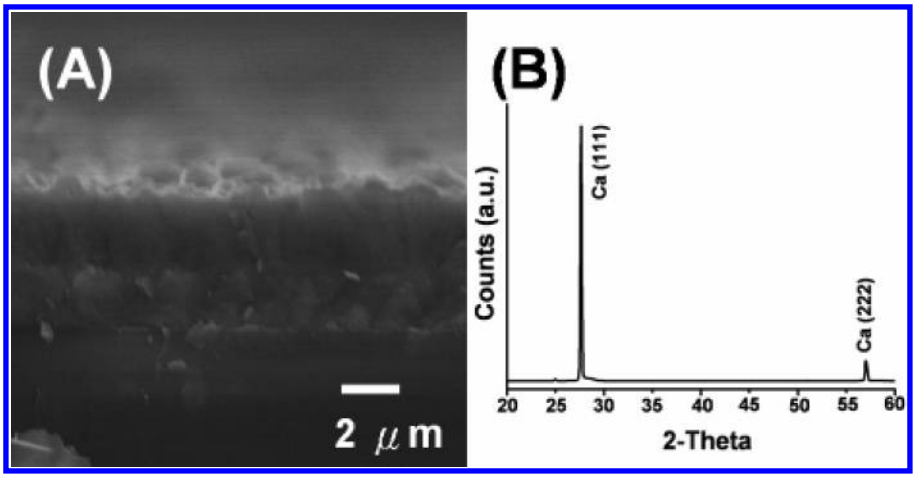

Figure 1. (A) Cross-sectional SEM image and (B) XRD pattern of a calcium thin film deposited on a Si substrate. The XRD pattern can be assigned to JCPDF no. 23-0423.

6330F at 15 kV. Transmission electron microscopy (TEM) and electron diffraction (ED) images were obtained on a JEOL JEM-2010 at 200 kV. High-resolution TEM (HRTEM) images were acquired on a JEOL JEM-4000EX at 400 kV. X-ray diffraction (XRD) studies were carried out using a BRUKER AXS D8 ADVANCE diffractometer using Cu $K\alpha_1$ radiation. Fourier transform infrared (FT-IR) spectra were carried out using a Perkin-Elmer Spectrum One. Thermal gravimetric analysis (TGA) was carried out on a Perkin-Elmer Diamond TGA.

Field emission measurements were performed in a vacuum chamber at a pressure of 1.05×10^{-3} Pa at room temperature. A 1 mm diameter spherical-shaped stainless-steel probe was used as the anode. Field emission characteristics of the samples were measured with a Keithley 237 (max output voltage 1100 V, current 10 mA). One sample of tubular SiC material on Si(100), which was grown at 873 K followed by heat treatment at 1273 K, was measured at an anode−sample distance of 65 μm while the applied field voltage was raised from zero to 940 V. Another sample of tubular SiC material on Si(100), which was grown at 923 K followed by heat treatment at 1273 K, was measured with at an anode−sample distance of 75 μm while the applied field voltage was raised from zero to 480 V. We define the turn-on field (E_{to}) and the threshold field (E_{th}) as the electric fields required to produce a current density of 10 μA cm^{-2} and 10 mA cm^{-2}, respectively.

Results and Discussion

The reaction was carried out in a horizontal hot-wall quartz tube reactor. Growth of a fresh surface Ca thin film with a thickness of approximately 5 μm on a Si(100) wafer at 430 K was achieved via a physical vapor deposition (PVD) process by evaporating Ca at 973 K. The Ca thin film, as characterized by SEM and XRD in Figure 1, was smooth and free from other crystalline phases, such as CaSi, $CaSi_2$, and CaO. At the deposition temperature, interdiffusion of elemental Ca and Si atoms to form $CaSi_x$ compounds was reported to be insignificant.[16] Then, the Ca thin film was reacted with vaporized $MeSiHCl_2$ at 773−923 K to form a solid precursor layer on Si. The layer was proposed to be $CaCl_2$ encapsulated inside a Yajima-type preceramic polycarbosilane precursor, SiC_xH_y.[12] The material was further

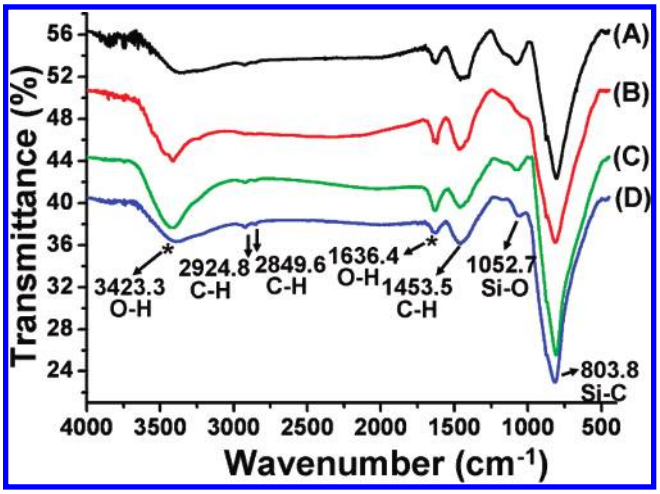

Figure 2. FT-IR spectra of samples grown at (A) 773 K, (B) 823 K, (C) 873 K, and (D) 923 K followed by heat treatment at 1273 K. The absorption bands marked with an asterisk (*) are from absorbed H_2O molecules.

processed at 1273 K under vacuum to thermally convert it into the final product. In the process, $CaCl_2$ was removed by evaporation as well. A yellow thin film, covering the Si substrate completely, was collected. For all thin films, the FT-IR data in Figure 2 show major absorptions from Si−C bonds near 800 cm^{-1} and minor ones from residual C−H bonds near 2925, 2850, and 1450 cm^{-1}.[12] XRD data displayed a broad peak at $2\theta = 35.7°$ from SiC(111) reflection (JCPDS no. 29-1129)[17] and sharp peaks from Si reflections (JCPDS no. 75-0589).[18] The samples were also characterized by using SEM, EDX, TEM, and selected area ED (SAED). With some variations in growth rates, sizes, and crystallinity, that is, they all increased with the increasing temperature of reaction, the products showed comparable morphology, composition, and microstructures. Typical observations will be discussed below.

SEM and XRD Characterizations. A low-magnification SEM image of the yellow thin film grown at 823 K on Si followed by heat treatment at 1273 K is shown in Figure 3A. The image displays numerous one-dimensional nano-

(16) (a) Canepa, F.; Napoletano, M.; Manfrinetti, P.; Palenzona, A. *J. Alloys Compd.* **2000**, *299*, 20. (b) Affronte, M.; Laborde, O.; Olcese, G. L.; Palenzona, A. *J. Alloys Compd.* **1998**, *274*, 68.

(17) Joint Committee for Powder Diffraction (JCPDS) File No. 75-0589. International Center for Diffraction Data, 1982.

(18) Joint Committee for Powder Diffraction (JCPDS) File No. 29-1129. International Center for Diffraction Data, 1982.

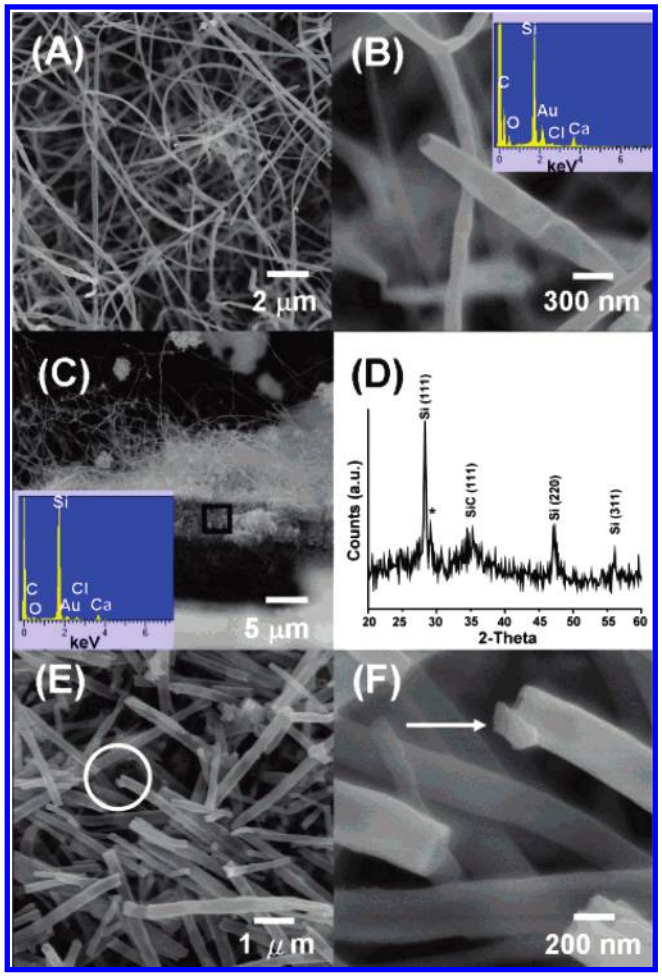

Figure 3. Characterization of a sample grown on Si wafer at 823 K followed by heat treatment at 1273 K. SEM studies: (A) low magnification surface image, (B) high magnification image of a tube end and EDX (inset, Au was sputtered to increase conductivity), (C) cross-sectional image of the deposited layers on Si and EDX (inset, from the squared area; Au was sputtered to increase conductivity), and (D) XRD pattern. The peak marked with an asterisk (*) is from the sample holder. (E) Low magnification image of tubes with ruptured ends and (F) high magnification of the circled area in part C showing a ruptured end of a sample grown on Si wafer at 873 K followed by heat treatment at 1273 K.

structures tens of micrometers long. High-magnification SEM images, such as the one in Figure 3B, suggest that the material has an apparently open-end tubular structure with a diameter of 100−200 nm. An EDX spectrum shown in Figure 3B (inset) indicates that the tubular material contains Si, C, and traces of Ca and Cl. An SEM image of the thin film/substrate cross section in Figure 3C reveals that the tubular nanomaterial layer has a thickness up to several tens of micrometers. In addition, an interlayer with a thickness of approximately 9 μm is observed between the tubular material layer and the Si substrate. An EDX spectrum of the interlayer, as shown in the inset of Figure 3C, indicates that the material contains more Si than the tubular material layer does.

Figure 3D shows the XRD pattern of the deposited layer after being removed from the Si substrate. The SiC(111) reflection and the Si reflections are observed.[18] By using the Scherrer equation, the crystallite sizes of SiC and Si are estimated to be 3 and 18 nm, respectively. Because only reflections of electrons from SiC were observed for the tube in the ED studies (to be discussed below), we suggest that the Si pattern in XRD was not from the tubular material layer. Instead, it might originate from the interlayer because it was Si rich as shown in the EDX result. One possible origin of the Si crystals was from residual fragments of the Si substrate. As the product layers were detached, some Si fragments might attach to the product and were removed together. Another possibility was that during the reaction between $MeSiHCl_2$ and Ca at 823 K, a $CaSi_x$ layer was also produced between the Ca thin film and the Si substrate by interdiffusion of the corresponding elements.[19] As the reaction progressed, the $CaSi_x$ layer might react with $MeSiHCl_2$ to generate the interlayer composed of SiC and Si. On the other hand, the presence of Si as a minor component in the tubular product layer was observed for samples deposited above 873 K (see below in TEM and TGA Studies). Even though the image in Figure 3B suggests that the one-dimensional material has an open-end tubular structure, another SEM image in Figure 3E shows a sample with many tubes with broken ends. An enlarged view in Figure 3F displays a ruptured tip of a one-dimensional structure.

TEM Studies. Figure 4A presents the TEM image of the sample grown at 823 K followed by heat treatment at 1273 K. It confirms that it is one-dimensional and has an apparent open-end tubular structure with a diameter of approximately 100 nm and a wall thickness of 10−20 nm. SAED reveals a slightly diffused pattern with three distinctive rings in Figure 4B suggesting that the sample is polycrystalline with crystallite sizes smaller than 4 nm. Starting from the most inside ring, these rings are assigned to the reflections from SiC(111), SiC(220), and SiC(311) planes. They can be assigned to cubic β-SiC with an estimated lattice parameter $a = 0.44$ nm.[17] No reflections from crystallites of Si and Ca containing solids can be seen. The observations are in good agreement with the XRD data. For the sample grown at 773 K followed by heat treatment at 1273 K, the TEM and ED data were comparable, showing an apparent open-end polycrystalline SiC tube with a diameter of approximately 80 nm and a wall thickness of 5−10 nm.

Figure 5A shows the TEM data of a sample deposited at 923 K and annealed at 1273 K. It is one-dimensional and open-end tubular with a diameter of approximetly 300 nm and a wall thickness of 60−80 nm. Only Si and C atoms can be observed in the EDX. SAED reveals a pattern with five distinctive rings in Figure 5B, suggesting that the sample is polycrystalline. They can be assigned to cubic Si with an estimated lattice parameter $a = 0.54$ nm and cubic β-SiC with an estimated lattice parameter $a = 0.44$ nm.[17,18] Starting from the most inside ring, these rings are assigned to the reflections from Si(111), SiC(111), Si(200), SiC(220), and SiC(311) planes. An HRTEM image, enlarged from the selected area in Figure 5A, is shown in Figure 5C. Two different lattice spacing values, 0.317 and 0.254 nm, are observed and assigned to the Si(111) and β-SiC(111) planes, respectively.[17,18] The Si content will be estimated using the TGA result discussed below. The possible sources of the Si crystallites are the following ones. The first is the extrusion of Si from the polymeric material within the preceramic

(19) Würz, R.; Schmidt, M.; Schöpke, A.; Fuhs, W. *Appl. Surf. Sci.* **2002**, *190*, 437.

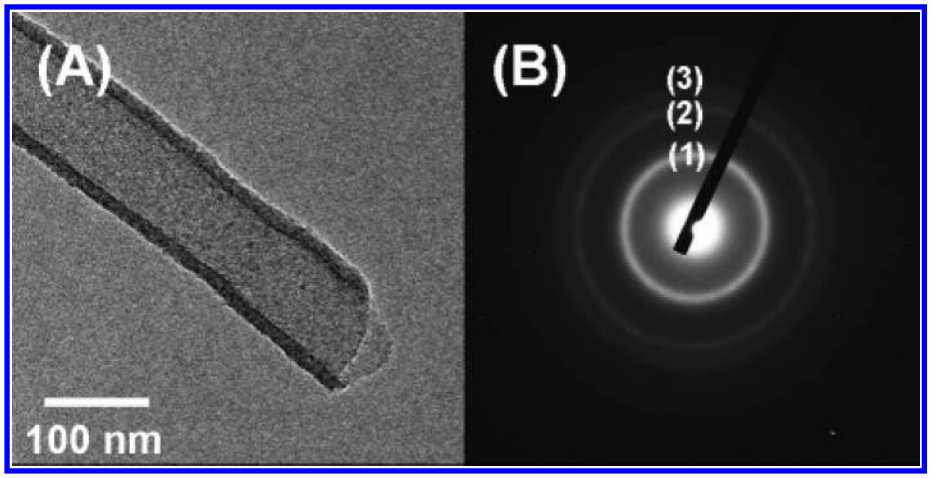

Figure 4. TEM studies of a sample grown at 823 K followed by heat treatment at 1273 K. (A) Low magnification image and (B) SAED.

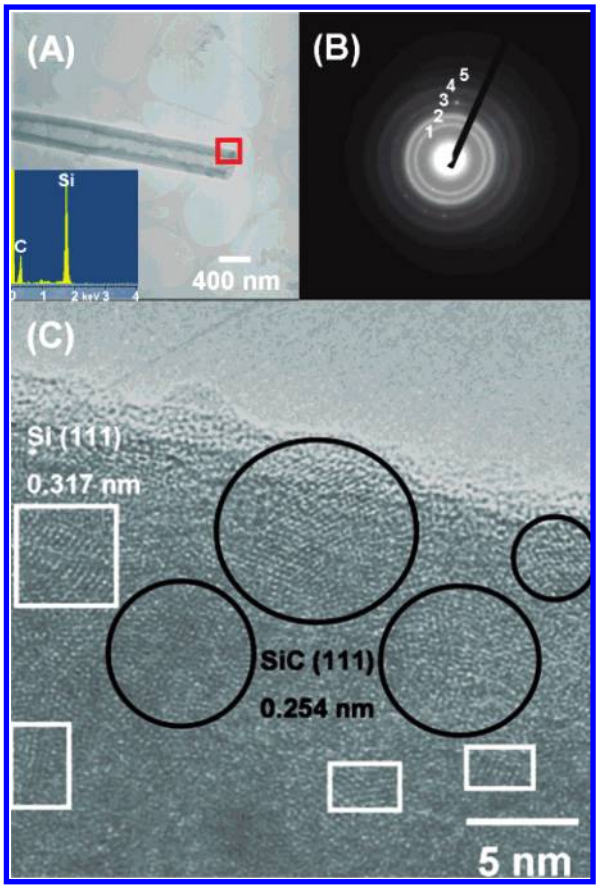

Figure 5. TEM studies of a sample grown at 923 K followed by heat treatment at 1273 K. (A) Low magnification image and EDX (inset, from the squared area). (B) SAED and (C) high-resolution image enlarged from a selected area in A.

precursor. In literature, in the preparation of β-SiC via the Yajima-type routes, this was frequently observed at the high-temperature processing stage.[12,20,21] Another possible source of Si is from the gas-phase decomposition of $MeSiHCl_2$.[22] It was reported that at 905 K, $MeSiHCl_2$ decomposed into CH_4 and $SiCl_2$ initially. Then, $SiCl_2$ was transformed into the final gas-phase products $HSiCl_3$ and $SiCl_4$. We propose that, in this study, these chlorosilanes may react with Ca to form the Si nanocrystals in the tubular walls.[23]

The data in Figure 6 suggest that the tubular structure was formed from an originally sealed heterostructure which ruptured later to allow the inner core to evaporate. The TEM image in Figure 6A shows a close examination of a tube with a ruptured end, which parallels to the SEM observations in Figure 3E,F. The presence of a core before the heat treatment is supported by the images of a rare example of a filled tube section shown in Figure 6B,D. The TEM image in Figure 6B reveals that the section is composed of Si, C, Ca, and Cl, as identified by the EDX in Figure 6C. By analyzing the ED pattern in Figure 6D carefully, we conclude that the sample contains β-SiC, Si, and $CaCl_2$. In the ED pattern, the polycrystalline diffraction rings 2, 5, and 6 are assigned to β-SiC while the rings 1, 3, and 4 are assigned to Si. The diffraction spots from single crystalline $CaCl_2$ are circled. On the basis of this and the observations discussed above, we suggest that the as-formed one-dimensional precursor material has a sealed radial heterostructure, which is composed of an inner core of $CaCl_2$ encapsulated inside a preceramic shell of SiC_xH_y. Later, during the high-temperature treatment at 1273 K, $CaCl_2$ vaporizes and raises the pressure inside the heterostructure. This would cause the originally sealed tips to rupture and allows $CaCl_2$ to evaporate. We expect that extended heat treatment should lower the $CaCl_2$ concentration further. Meanwhile, SiC crystallizes inside the shell to form the apparent open-end tube morphology.

TGA Studies. From the above discussions, it is reasonable to assume that the tubular products are composed of β-SiC mainly. Silicon appears to be a minor component. In addition, the samples may contain amorphous SiC (a-SiC) and amorphous C (a-C). To understand the stability and composition of the products, they were analyzed by TGA in an ambiance of 100 sccm of flowing air. For the sample grown at 923 K followed by heat treatment at 1273 K, it showed 5% weight loss at 873 K. This was due to the oxidation of

(20) (a) Bianconi, P. A.; Weidman, T. W. *J. Am. Chem. Soc.* **1989**, *110*, 2342. (b) Bianconi, P. A.; Schilling, F. C.; Weidman, T. W. *Macromolecules* **1989**, *22*, 1697.
(21) Seyferth, D.; Wood, T. G.; Tracy, H. J.; Robison, J. I. *J. Am. Ceram. Soc.* **1992**, *75*, 1300.
(22) Ring, M. A.; O'Neal, H. E.; Walker, K. L. *Int. J. Chem. Kinet.* **1998**, *30*, 89.
(23) Huang, C.-H.; Chang, Y.-H.; Lin, H.-K.; Peng, C.-H.; Chung, W.- S.; Lee, C.-Y.; Chiu, H.-T. *J. Phys. Chem. C* **2007**, *111*, 4138.

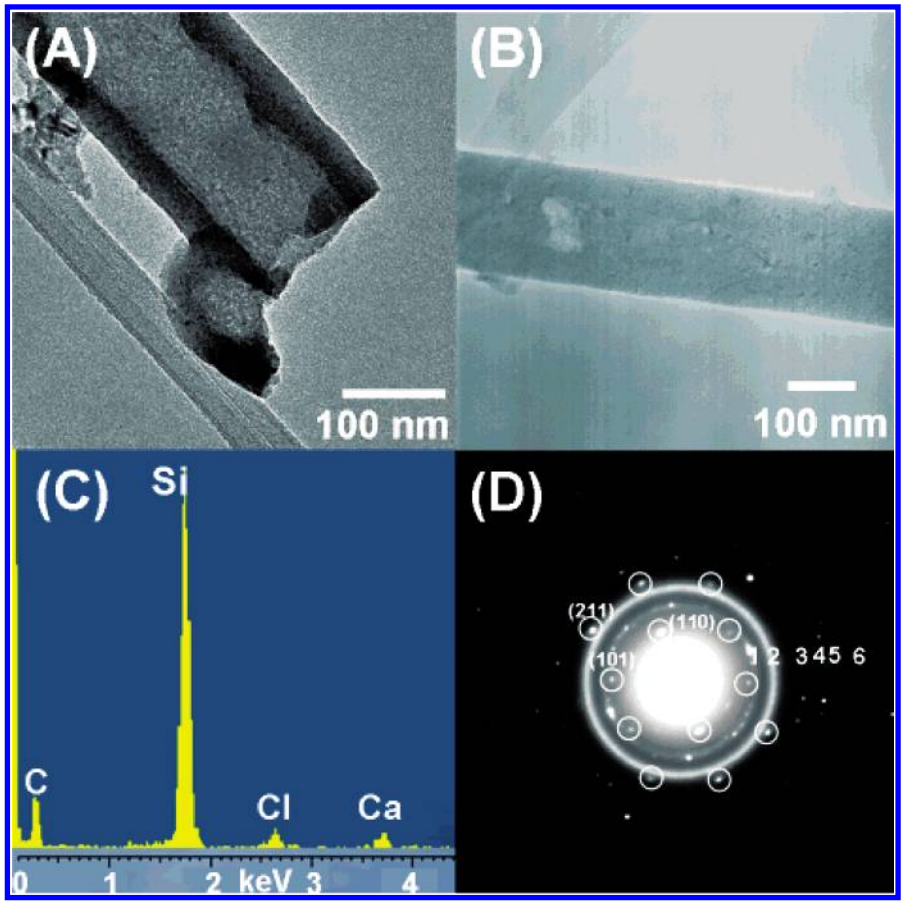

Figure 6. (A) TEM image of a sample grown at 873 K followed by heat treatment at 1273 K showing a tube end. (B) TEM image, (C) EDX, and (D) ED pattern of a sample grown at 923 K followed by heat treatment at 1273 K still retaining the $CaCl_2$ core.

carbon atoms in the sample to form volatile CO_2. Bulk β-SiC is known for its resistance to air oxidation at high temperatures.[24] *a*-SiC may be oxidized more easily, but the weight should be increased instead of lowered. Thus, the only origin of weight loss is the oxidation of *a*-C. As the temperature increased from 873 to 1273 K, the weight increased 8%. Then, as the sample was heated at 1273 K for 10 min, the weight increased 2%. Finally, after the temperature was lowered to 425 K, another 3% weight increase was observed. We attribute the 13% weight increase, starting at 873 K, to the oxidation of *a*-SiC and Si in the sample to form SiO_2. $HSiCl_3$ and $SiCl_4$, generated from the dissociation of $MeSiHCl_2$, are the probable sources of Si.[22] The final weight was 108% of the initial sample weight. By assuming that only *a*-C was oxidized below 873 K, we employed the trial and error method to estimate possible tube compositions. If the sample does not contain any *a*-SiC, its composition is 84% β-SiC, 11% Si, and 5% *a*-C by weight. This corresponds to an atomic composition of 72% β-SiC, 14% Si, and 14% *a*-C. It is possible that the sample contains some *a*-SiC. For example, if the weight of *a*-SiC is 2% and the amount of *a*-C is the same 5%, there is 83% β-SiC and 10% Si. The atomic composition of the sample is determined to be 72% β-SiC, 2% *a*-SiC, 12% Si, and 14% *a*-C. Another estimation shows that if the sample contains 8% *a*-SiC and 5% *a*-C by weight, there is 79% β-SiC and 8% Si. This corresponds to an atomic composition of 69% β-SiC, 10% *a*-SiC, 7% Si, and 14% *a*-C.

A similar TGA study and data analysis was performed for the sample grown at 823 K followed by heat treatment at 1273 K. At 823 K, the decomposition of $MeSiHCl_2$ into $HSiCl_3$ and $SiCl_4$ is insignificant.[22] The sample probably contained a reasonably high amount of *a*-SiC but much less Si. For the first example, we assume that the sample did not have Si at all. If so, the atomic composition is estimated to be 46% β-SiC, 34% *a*-SiC, and 20% *a*-C. Another example assumes that the sample contains some Si, 5% by weight. Under this condition, the possible atomic composition is estimated to be 49% β-SiC, 25% *a*-SiC, 6% Si, and 20% *a*-C. Another estimated atomic composition, with 14% Si by weight, is 58% β-SiC, 7% *a*-SiC, 16% Si, and 19% *a*-C. On the basis of the analyses, we conclude that SiC, including β-SiC and *a*-SiC, was the major component in the tubular products. The Si content in the samples should be far less than 20%. It is important to note that the temperature of reaction affected the ceramic precursor structure and composition significantly. The higher reaction temperature produced better mixed and bonded SiC precursor. In turn, after the heat treatment, the better precursor generated a better final product, containing more crystallized β-SiC.

Proposed Reaction Pathway. On the basis of the above information, we propose in Scheme 1 a pathway to summarize the overall reaction steps. We suggest that the SiC tubes are grown via a VSRG pathway similar to the one

(24) Narushima, T.; Goto, T.; Iguchi, Y.; Hirai, T. *J. Am. Ceram. Soc.* **1990**, *73*, 3580.

Scheme 1. Reaction Steps To Form Tubular SiC on the Si Wafer

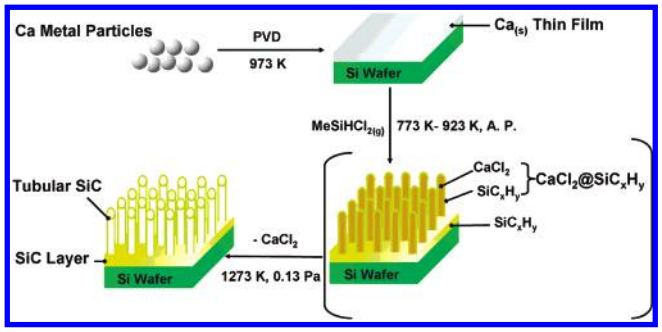

proposed before for the growth of one-dimensional radial heterostructure composed of a CaF_2 core and an *a*-C shell.[9] In the current study, the reaction between $MeSiHCl_2$ and Ca produced phase segregated radial heterostructure of $CaCl_2$ and SiC_xH_y on the substrate. The ionic $CaCl_2$, as a result of a high cohesive force, forms an inner core. In addition, because the reaction temperature employed in this study, 773−923 K, is significantly lower than the melting point of $CaCl_2$, 1048 K, $CaCl_2$ can only grow into small diameter seeds at the early growth stage. The seeds are wrapped inside the other product, soft polymeric shells of SiC_xH_y, which are also formed at the vapor−solid reaction interface. Because the inner seed diameter is restricted by the polymeric shell, incorporation of more products to the composite seed does not enlarge it isotropically but elongate it in one dimension. These factors work cooperatively to develop the products into a closed-end cable-like radial heterostructure composed of a $CaCl_2$ core and a SiC_xH_y shell. Then, at an elevated temperature under vacuum, the preceramic shell is transformed into SiC nanocrystals while the $CaCl_2$ core evaporates and erupts from the cable ends. This would generate the tubes with the apparent open-end morphology.

Field Emission Property Studies. Field emission property of the tubes is evaluated.[25] As shown in Figure 7A, a sample grown on Si(100) at 873 K followed by heat treatment at 1273 K shows an excellent emission property E_{to} (turn-on field) of 2.8 V/μm and E_{th} (threshold field) exceeding 16 V/μm. Another sample, deposited at 923 K followed by heat treatment at 1273 K, showed an E_{to} of 2.5 V/μm and E_{th} of less than 7 V/μm in Figure 7B. Clearly, the tubes grown at 923 K performed better than the ones grown at 873 K, even though they were heat-treated at the same temperature of 1273 K. For both samples, the Fowler−Nordheim plots of the curves showed linear sections above E_{to}. This suggests that their field emission mechanism is conventional.[26] It is known that the field enhancement factor, β, is strongly dependent on the sample geometry.[27,28] Generally, samples with high one-dimensional aspect ratio structures showed low turn on values.[29,30] In this study, employing a work function

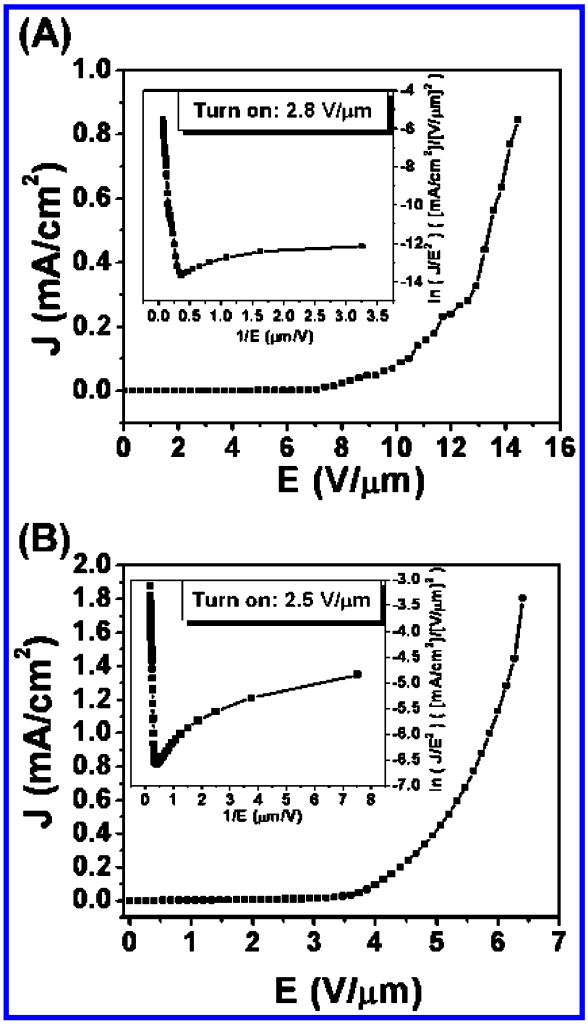

Figure 7. Field emission $J-E$ curve and Fowler−Nordheim (F−N) plot (inset). (A) A tubular SiC material on Si(100) at 873 K and heat treated at 1273 K. (B) A tubular SiC material on Si(100) at 923 K and heat treated at 1273 K.

(Φ) value of 4.4 eV for SiC and slopes of the F−N plots in the insets in Figure 5, the β values are estimated to be 1800 and 2900 for the samples grown at 873 and 923 K, respectively.[31] The reason why that the tubes grown at 923 K performed better, emitting higher current at lower field, is attributed to the higher content of crystallized β-SiC in the product. As far as we know, the results discussed above are the first field emission property data for SiC tubes. The data are much lower than most of the reported data of other SiC nanostructures.[29−32]

Conclusions

In this study, we have synthesized SiC tubes via a VSRG pathway employing the vapor of $MeSiHCl_2$ to react with Ca deposited on Si. The reaction is a solvent-free Yajima-type process that takes place at the vapor−solid interface. For

(25) Lee, Y.-C.; Pradhan, D.; Lin, S.-J.; Chia, C.-T.; Cheng, H.-F.; Lin, I.-N. *Diamond Relat. Mater.* **2005**, *14*, 2055.
(26) Fowler, R. H.; Nordheim, L. W. *Proc. R. Soc. London, Ser. A* **1928**, *119*, 173.
(27) Yamanaka, T.; Tampo, H.; Yamada, K.; Ohnishi, K.; Hashimoto, M.; Asahi, H. *Phys. Status Solidi C* **2002**, *1*, 469.
(28) Lee, C. J.; Lee, T. J.; Lyu, S. C.; Zhang, Y.; Ruh, H.; Lee, H. J. *Appl. Phys. Lett.* **2002**, *81*, 3648.
(29) Shen, G.; Bando, Y.; Ye, C.; Liu, B.; Golberg, D. *Nanotechnology* **2006**, *17*, 3468.
(30) Deng, S. Z.; Li, B. Z.; Wang, W. L.; Xu, N. S.; Zhou, J.; Zheng, X. G.; Xu, H. T.; Chen, J.; She, J. C. *Appl. Phys. Lett.* **2006**, *89*, 23118.
(31) Wu, Z. S.; Deng, S. Z.; Xu, N. S.; Chen, J.; Zhou, J.; Chen, J. *Appl. Phys. Lett.* **2002**, *80*, 3829.
(32) Zhou, X. T.; Lai, H. L.; Peng, H. Y.; Au, F. C. K.; Liao, L. S.; Wang, N.; Bello, I.; Lee, C. S.; Lee, S. T. *Chem. Phys. Lett.* **2000**, *318*, 58.

the reaction, the products $CaCl_2$ and SiC_xH_y phase-segregate and undergo transformation into a cable-like radial heterostructure. After heat treatment, which converts the preceramic SiC_xH_y shell material into SiC and removes the $CaCl_2$ core, the layer of SiC tubes is fabricated on Si. From the tubes, emission of electrons with a current 10 $\mu A/cm^2$ can be obtained at an applied field as low as 2.5 V/μm. We suggest that the high performance is not only due to the high aspect ratio of the one-dimensional tubular morphology but also to the large field enhancing factor β. This excellent result indicates that the SiC tubes may have promising field-emitting applications for vacuum microelectronic devices.

Acknowledgment. We are grateful to the supports from the National Science Council and the Ministry of Education of Taiwan, the Republic of China.

Supporting Information Available: XRD, SEM, EDX, TEM, ED, TGA, and composition analysis data (PDF). This material is available free of charge via the Internet at http://pubs.acs.org.

CM070925E